

Molecular Characterization of PDCBT

Nuclear Magnetic Resonance (NMR) experiments were carried out using a Bruker Advance 400 spectrometer. All chemical shifts were reported in the standard notation of parts per million (ppm) using the peak of residual proton signal of TCE-d₂ (δ =5.94 ppm).

¹H-NMR (TCE-d₂, 400 MHz, ppm) δ : 7.47-7.40 (m, 4H), 7.13-7.05 (m, 2H), 4.13 (d, 4H), 1.66 (s, 2H), 1.35-1.15 (br, 32H), 0.84-0.75 (br, 12H).

Size Exclusion Chromatography (SEC) measurements using *ortho*-dichlorobenzene (*o*-DCB) as mobile phase at high temperature were carried out by using an integrated GPCV2000 SEC system (Waters Corp., Milford, MA, USA) equipped with a differential refractometer (DRI) as concentration detector. In order to avoid the thermal degradation and the formation of aggregates, the samples were prepared with an optimized procedure, as follows: *i*) protection with butylated hydroxytoluene (BHT) antioxidant (0.05%); *ii*) samples solubilization in oven at 140 °C for about one hour; *iii*) filtration with sintered metal filters of 0.5 μ m pores size; *iv*) insertion of the samples in the injection compartment of the system at 135 °C.

HT-SEC: M_n = 16790 g·mol⁻¹; M_w = 36540 g·mol⁻¹; M_w/M_n = 2.2.

Photophysical characterization of PDCBT and PDCBT-based WPNPs

Photoluminescence (PL) spectra and Photoluminescence Excitation (PLE) profiles were obtained with NanoLog composed by an iH320 spectrograph equipped with a Synapse QExtra charge-coupled device, by exciting with a monochromate 450W Xe lamp. The spectra are corrected for the instrument response. PL Quantum Yield (PLQY) values of solutions were obtained by using Rhodamine 101 as the reference. Time-correlated single photon counting (TCSPC) measurements were obtained with PPD-850 single photon detector module by exciting with DD-405L DeltaDiode Laser and analysed with the instrument software DAS6.

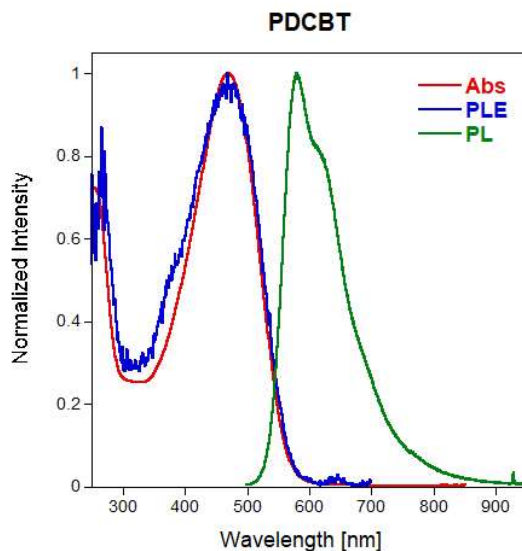


Figure S1. Absorption (red), emission (green) and excitation profiles (blue) spectra of PDCBT.

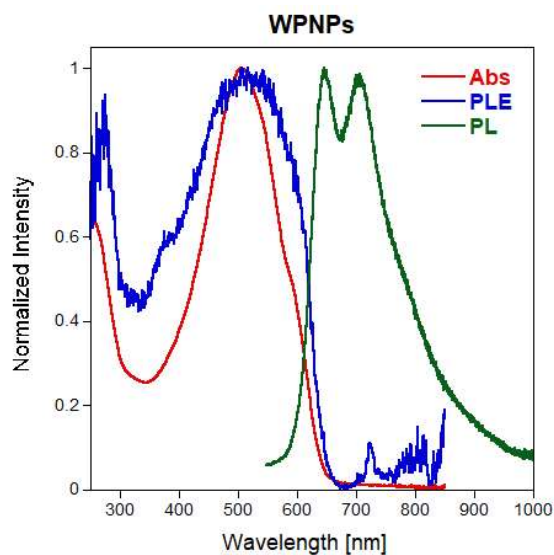


Figure S2. Absorption (red), emission (green) and excitation profiles (blue) spectra of PDCBT-based WPNPs.

Sample	$\lambda_{\text{abs-max}}$ (abs range) [nm]	PLE range [nm]	$\lambda_{\text{em-max}}$ [nm]	QY [%]
PDCBT	470 (340-540)	340-540	580 (shoulder at 615)	24
WPNPs	505 (375-610)	335-620	645, 705	4.5

Table S1. Photophysical properties of PDCBT and PDCBT-based WPNPs.

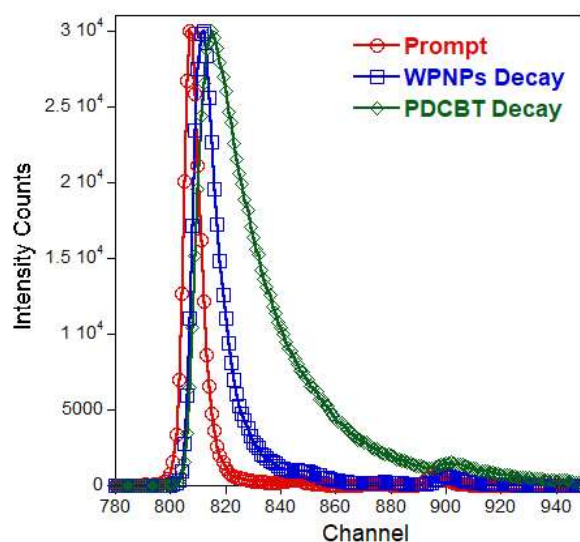


Figure S3. PL decays of PDCBT (green) and PDCBT-based WPNPs (blue), measured at 575 nm and 645, respectively, together with the laser response (red).

Sample	τ_1 [ps]	τ_2 [ps]	A_1	A_2	τ_{avg} [ps]
PDCBT	180	600	0.11	0.89	554
WPNPs	320	69	0.31	0.69	147

Table S2. PL decays of PDCBT and WPNPs measured at 575 nm and 615 nm, respectively, by exciting at 407 nm. For the calculations bi-exponential fits have been considered.

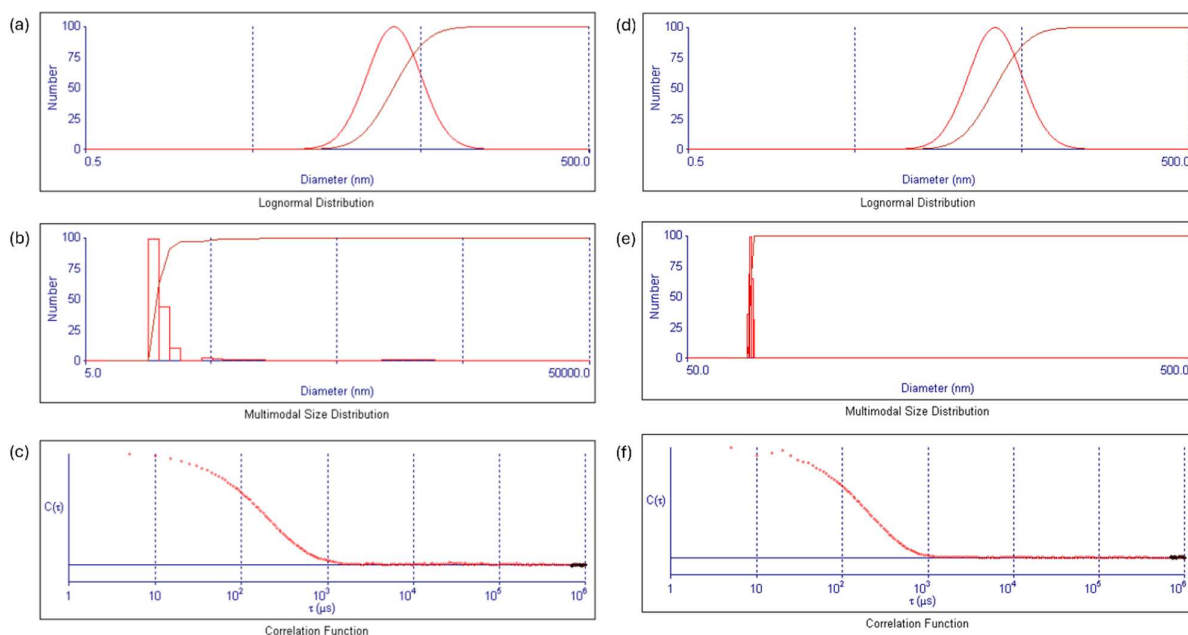


Figure S4. (a) DLS lognormal distribution by number of diameters, (b) multimodal size distribution by number and (c) correlation function of sample CPNP58B and (d) DLS lognormal distribution by number of diameters, (e) multimodal size distribution by number and (f) correlation function of sample CPNP64.

Sample	Mean Diameter [nm]	PDI
CPNP58B	36.80	0.16
CPNP64	70.00	0.09

Table S3. Mean diameter and Polydispersity Index of samples CPNP58B and CPNP64.

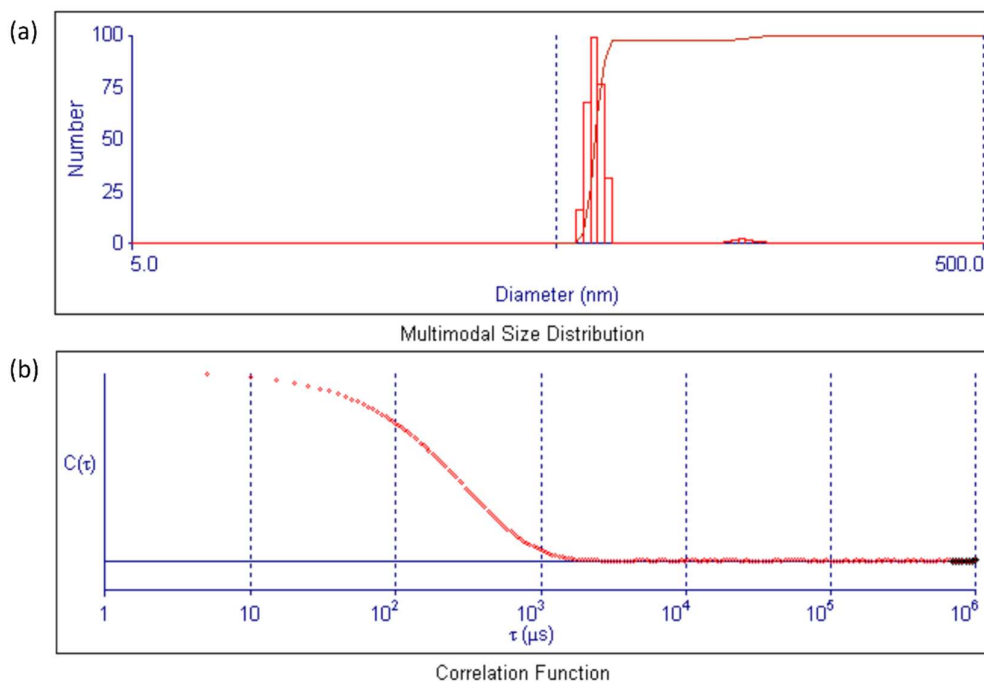


Figure S5. DLS data of PDCBT WPNP suspension: (a) multimodal size distribution by number and (b) correlation function.

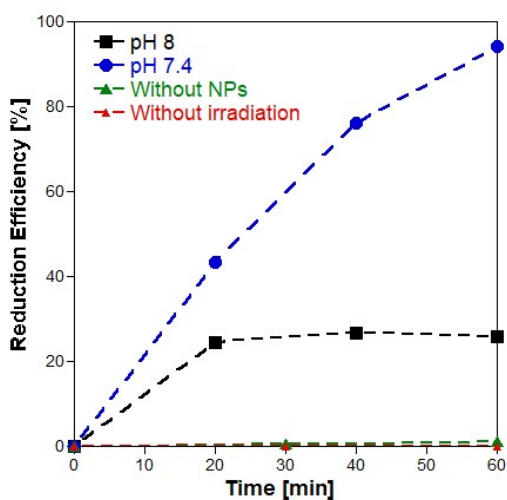


Figure S6. Time dependence of the regeneration efficiency changes of MV^{2+} produced in the system containing TEOA, WPNPs and MV^{2+} without irradiation (red triangles) and upon 60-minute-irradiation at pH 8 (black squares), pH 7.4 (blue circles) and without nanoparticles (green triangles).

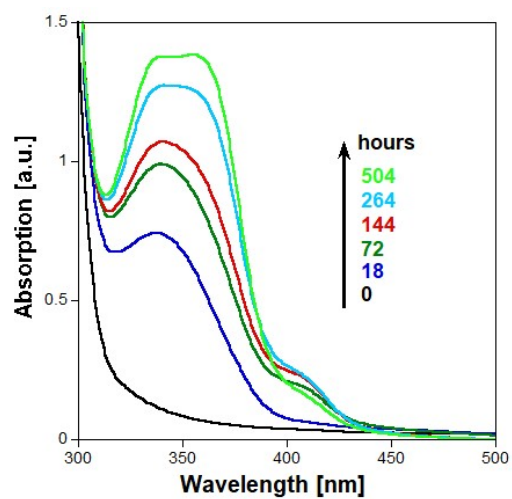


Figure S7. Absorption spectra changes of the suspension containing TEOA, PDCBT WPNPs, MV^{+} , NAD^{+} and $NaHCO_3$ over time.

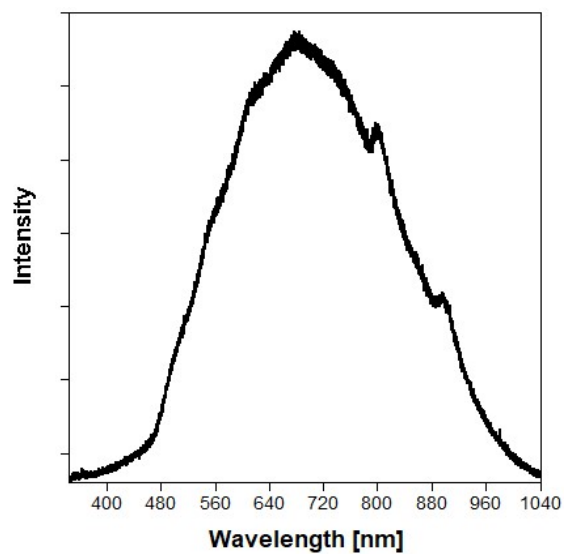


Figure S8. Spectral profile of the applied light source.

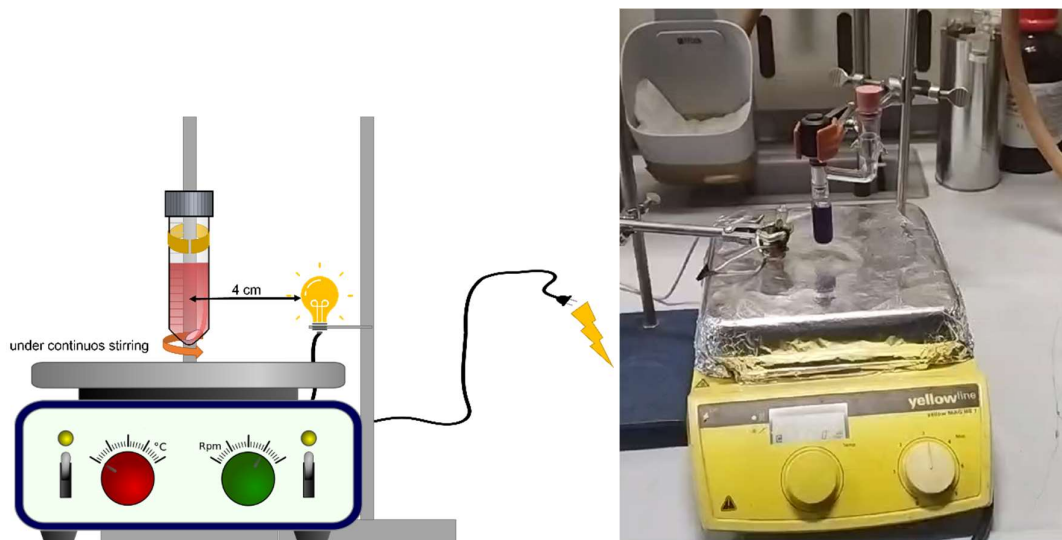


Figure S9. Experimental setup.

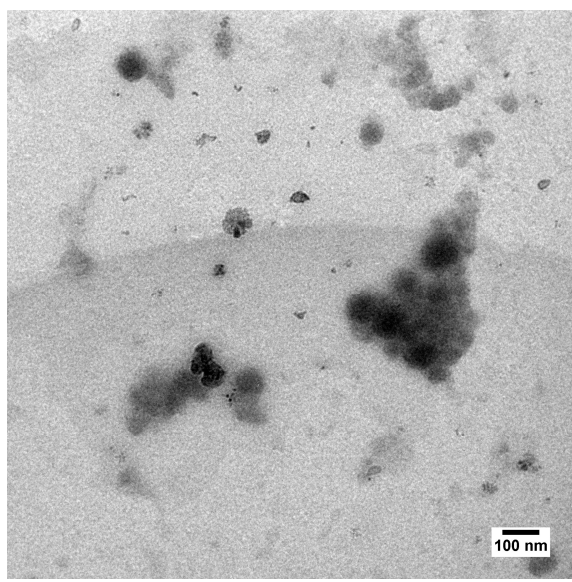


Figure S10. TEM Image of WPNPs: the image is blurry because of the presence of surfactant around the WPNPs.

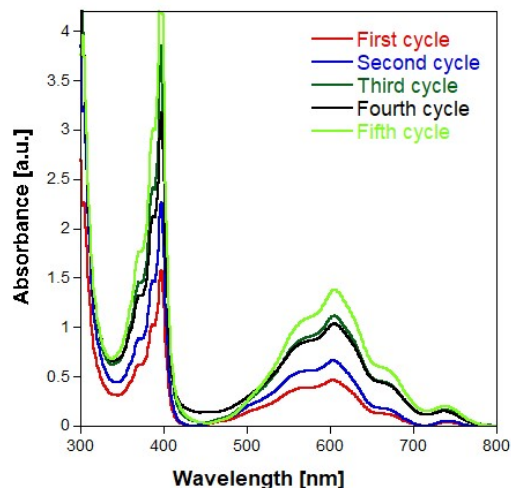


Figure S11. Absorption spectra of the suspensions containing TEOA, PDCBT WPNPs and $MV^{\bullet+}$ over five consecutive photocatalytic cycles.

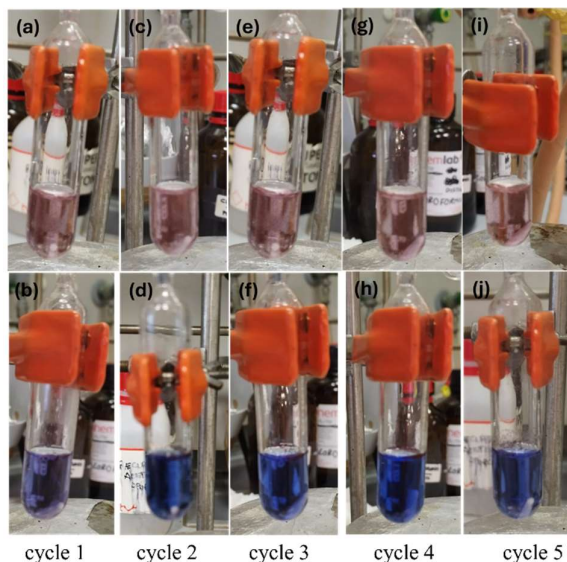


Figura S12. Pictures of the reaction solution before (a) and after (b) the first photocatalytic cycle; before (c) and after (d) the second photocatalytic cycle; before (e) and after (f) the third photocatalytic cycle; before (g) and after (h) the fourth photocatalytic cycle; before (i) and after (j) the last photocatalytic cycle. The color change indicates the successful reduction of methyl viologen ($MV^{\bullet+}$) and demonstrates the sustained activity of the photocatalyst over multiple cycles.

References

- [1] R. Heuvel, F. J. M. Colberts, M. M. Wienk, R. A. J. Janssen, *J. Mater. Chem. C* **2018**, *6*, 3731.
- [2] M. Diterlizzi, Polymeric Water-Processable Nanoparticles towards Sustainable Organic Photovoltaics, Università degli Studi Milano-Bicocca, **2022**.